

## Buckling of thin-walled members analyzed by Mindlin-Reissner finite strip

Bui H. Cuong\*

*Department of Civil and Industrial Building, National University of Civil Engineering,  
55 Giai Phong Street, Ha noi, Vietnam*

*(Received August 3, 2012, Revised September 7, 2013, Accepted September 18, 2013)*

**Abstract.** The paper presents the formulation of 3-nodal line semi-analytical Mindlin-Reissner finite strip in the buckling analysis of thin-walled members, which are subjected to arbitrary loads. The finite strip is simply supported in two opposite edges. The general loading and in-plane rotation techniques are used to develop this finite strip. The linear stiffness matrix and the geometric stiffness matrix of the finite strip are given in explicit forms. To validate the proposed model and study its performance, numerical examples of some thin-walled sections have been performed and the results obtained have been compared with finite element models and the published ones.

**Keywords:** finite strip; buckling analysis; arbitrary load; general loading condition; Mindlin plate theory; Mindlin-Reissner finite strip

### 1. Introduction

The semi-analytical finite strip method is based on the harmonics functions, and proved to be an efficient tool for analysing prismatic structures. This method was pioneered by Cheung (1976), who used the classical plate theory of Kirchhoff. Many authors have adopted and extended this method to analyse thin-walled sections. Hancock (1978) presented the buckling curve of a thin-walled I-section. This relates to buckling stress with half-wave lengths and enables a better insight into the elastic stability of a section. The distortional buckling phenomenon is also better understood. The semi-analytical finite strip method is also applied in the nonlinear elastic and elastic-plastic studies (Bradford and Hancock 1984, Key and Hancock 1993, Ovesy *et al.* 2005, Ovesy *et al.* 2006, Ovesy *et al.* 2006, Milašinović 2011).

The semi-analytical finite strip method can be also based on the Mindlin-Reissner flat shell theory. The latter allows the shear effect to be calculated through the plate thickness. Hinton (1978) highlighted the dependence of the normalised critical stress on the thickness of isolated plates. Dawe *et al.* (1993), Wang and Dawe (1996) analysed the nonlinear elastic response of thin-walled sections. The local and global behaviour is separately examined. Zahari and El-Zafrany (2009) considered the progressive failure of composite laminated stiffened plates. Bui and Rondal (2008) studied the buckling behaviour of highly stiffened thin-walled sections, for which the

---

\*Corresponding author, Ph.D., E-mail: [bhungcuong@gmail.com](mailto:bhungcuong@gmail.com)

Mindlin-Reissner finite strips are better than the Kirchhoff ones.

In the buckling analysis, most of the above works are limited to the members subjected to uniform compression or uniform bending or the combination of these two loading cases. Chu *et al.* (2005), Chu *et al.* (2006) examined a particular case, where stresses vary along the longitudinal axis of cold-formed sections under uniform distributed loads, which are applied at the shear centre. Bui (2009) established the formulation of 2-nodal line semi-analytical finite strip based on the Kirchhoff plate theory, this strip can analyse the buckling of thin-walled sections under general loading conditions.

The objective of this paper is the application the approaches proposed in the previous works (Bui and Rondal 2008, Bui 2009) to develop a semi-analytical finite strip based on the Mindlin-Reissner flat shell theory. For a general loading condition, we proposed realizing linear analysis first to give longitudinal stresses. The linear stiffness matrix is provided in the standard manner. Each strip is divided into cells and longitudinal stresses are recorded in these cells. The integrations are performed on each cell domain and the sum of them provides the geometric matrix of the strip. This work is limited in a linear buckling analysis, effects of the pre-deflection on stability of thin-walled beams in a non-linear model are not considered here. This issue can be found in a study of Mohri *et al.* (2012), among others.

## 2. Deformation-displacement relation

The deformation-displacement relation in the Mindlin-Reissner finite strip can be predicted by the combination of the plane elasticity and the Mindlin plate theory

$$\begin{aligned}
 \varepsilon_x &= \frac{\partial u}{\partial x} - z \frac{\partial \theta_y}{\partial x} & \gamma_{xz} &= \frac{\partial w}{\partial x} - \theta_y \\
 \varepsilon_y &= \frac{\partial v}{\partial y} - z \frac{\partial \theta_x}{\partial y} & \gamma_{yz} &= \frac{\partial w}{\partial y} - \theta_x \\
 \gamma_{xy} &= \left( \frac{\partial u}{\partial y} - z \frac{\partial \theta_y}{\partial y} \right) + \left( \frac{\partial v}{\partial x} - z \frac{\partial \theta_x}{\partial x} \right)
 \end{aligned} \tag{1}$$

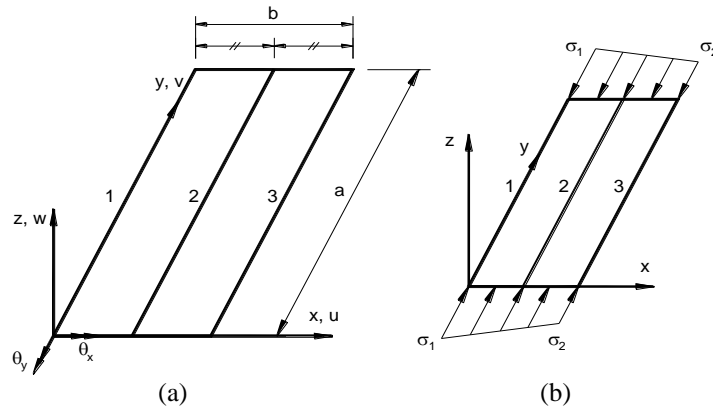


Fig. 1 (a) 3-nodal line Mindlin-Reissner finite strip; (b) strip with edge traction

where  $u$ ,  $v$  and  $w$  are the displacements in the  $x$ ,  $y$  and  $z$  directions;  $\theta_x$  and  $\theta_y$  represent rotations of the mid-surface normal in the  $yz$  and  $xz$ -planes, respectively and they are presented by double-arrow in Fig. 1(a).

### 3. Formulation

#### 3.1 Displacement functions

The three displacements and two rotations of the strip at a point  $(x,y)$  can be expressed as

$$\begin{aligned} u &= \sum_{m=1}^r \sum_{i=1}^n H_i u_i^m \sin \frac{m\pi y}{a} & \theta_x &= \sum_{m=1}^r \sum_{i=1}^n H_i \theta_{xi}^m \cos \frac{m\pi y}{a} \\ v &= \sum_{m=1}^r \sum_{i=1}^n H_i v_i^m \cos \frac{m\pi y}{a} & \theta_y &= \sum_{m=1}^r \sum_{i=1}^n H_i \theta_{yi}^m \sin \frac{m\pi y}{a} \\ w &= \sum_{m=1}^r \sum_{i=1}^n H_i w_i^m \sin \frac{m\pi y}{a} \end{aligned} \quad (2)$$

in which the chosen longitudinal harmonic functions are the classic ‘simply supported’ boundary conditions;  $r$  is the number of harmonics considered and  $n$  is the number of polynomial shape functions.

For 3-nodal line strip (Fig. 1(a))

$$H_1 = 1 - \frac{3x}{b} + \frac{2x^2}{b^2}, \quad H_2 = \frac{4x}{b} - \frac{4x^2}{b^2}, \quad H_3 = \frac{-x}{b} + \frac{2x^2}{b^2} \quad (3)$$

#### 3.2 Linear stiffness matrix of a strip

The linear stiffness of a strip can be derived from the strain energy

$$U = \frac{1}{2} \int_{-t/2}^{t/2} \int_A \{\boldsymbol{\varepsilon}_p\}^T [D_p] \{\boldsymbol{\varepsilon}_p\} d(\text{area}) dz + \frac{\kappa}{2} t \int_A \{\boldsymbol{\varepsilon}_s\}^T [D_s] \{\boldsymbol{\varepsilon}_s\} d(\text{area}) \quad (4)$$

where  $\kappa$  is the shear corrective factor ( $\kappa=5/6$ ).

$\{\boldsymbol{\varepsilon}_p\}$  and  $\{\boldsymbol{\varepsilon}_s\}$  represent the in-plane and out-of-plane shear strains, respectively, which are given by Eq. (1)

$$\{\boldsymbol{\varepsilon}_p\}^T = \{\boldsymbol{\varepsilon}_x \quad \boldsymbol{\varepsilon}_y \quad \boldsymbol{\gamma}_{xy}\} \quad (5)$$

$$\{\boldsymbol{\varepsilon}_s\}^T = \{\boldsymbol{\gamma}_{xz} \quad \boldsymbol{\gamma}_{yz}\} \quad (6)$$

$[D_p]$  and  $[D_s]$  are the elasticity matrices.

$$[D_p] = \frac{E}{1-\nu^2} \begin{bmatrix} 1 & \nu & 0 \\ \nu & 1 & 0 \\ 0 & 0 & \frac{1-\nu}{2} \end{bmatrix} \quad (7)$$

$$[D_s] = \begin{bmatrix} G & 0 \\ 0 & G \end{bmatrix} \quad \text{with} \quad G = \frac{E}{2(1+\nu)} \quad (8)$$

The in-plane and out-of-plane shear strains can be calculated by substituting Eq. (2) into Eq. (1)

$$\{\varepsilon_p\} = \sum_{m=1}^r [B_p^m] \{\delta^m\} \quad (9)$$

$$\{\varepsilon_s\} = \sum_{m=1}^r [B_s^m] \{\delta^m\} \quad (10)$$

in which, typical terms for nodal line  $i$  and  $m^{\text{th}}$  harmonic can be written as

$$[B_{pi}^m] = \begin{bmatrix} H_{i,x} s^m & 0 & 0 & 0 & -z H_{i,x} s^m \\ 0 & -H_i k^m s^m & 0 & z H_i k^m s^m & 0 \\ H_i k^m c^m & H_{i,x} c^m & 0 & -z H_{i,x} c^m & -z H_i k^m c^m \end{bmatrix} \quad (11)$$

$$[B_{si}^m] = \begin{bmatrix} 0 & 0 & H_{i,x} s^m & 0 & -H_i s^m \\ 0 & 0 & H_i k^m c^m & -H_i c^m & 0 \end{bmatrix} \quad (12)$$

where

$$H_i = H_i(x) ; H_{i,x} = \frac{dH_i(x)}{dx} ; k^m = \frac{m\pi}{a} ; s^m = \sin(k^m y) ; c^m = \cos(k^m y) \quad (13)$$

The nodal displacements for nodal line  $i$  and  $m^{\text{th}}$  harmonic is written as

$$\{\delta_i^m\}^T = \{u_i^m \quad v_i^m \quad w_i^m \quad \theta_{xi}^m \quad \theta_{yi}^m\} \quad (14)$$

The linear stiffness matrix of the strip can be obtained by substituting Eqs. (9) and (10) into Eq. (4). Note that, for simply supported strips, each harmonic term is uncoupled and thus the global stiffness matrix consists of  $r$  sub-stiffness matrices, which have a diagonal location

$$[K]_e = \begin{bmatrix} [K^1]_e & 0 & \dots & 0 \\ 0 & [K^2]_e & \dots & 0 \\ \dots & \dots & \dots & \dots \\ 0 & 0 & \dots & [K^r]_e \end{bmatrix} \quad (15)$$

in which the  $m^{\text{th}}$  sub-matrix can be given by

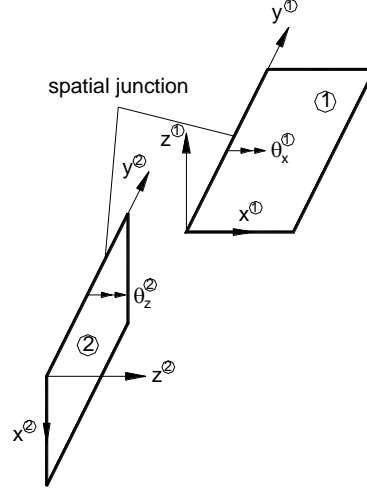


Fig. 2 Conformity of rotations at a spatial junction

$$[K^m]_e = \int_{-t/2}^{t/2} \int_A [B_p^m]^T [D_p] [B_p^m] d(\text{area}) dz + \kappa t \int_A [B_s^m]^T [D_s] [B_s^m] d(\text{area}) \quad (16)$$

### 3.3 In-plane rotation

The in-plane rotation problem can arise when the semi-analytical Mindlin-Reissner finite strip is used in analysing thin-walled sections. Bui and Rondal (2008) have proposed a technique to fix this problem, in which a fictitious in-plane shear strain concerning in-plane rotation is added in the standard deformation-displacement relation of the Mindlin-Reissner flat shell theory. Once the in-plane rotation was added, the conformity of rotations at a spatial junction of thin-walled section is assured as shown in Fig. 2. Consequently, fictitious stiffness associated with nodal in-plane rotations can be provided and this stiffness does not depend on harmonic terms. We rewrite here the fictitious stiffness for the 3-nodal line strip

$$\frac{1}{360} tabG \begin{bmatrix} 19 & -8 & -11 \\ -8 & 16 & -8 \\ -11 & -8 & 19 \end{bmatrix} \begin{bmatrix} \theta_{z1}^m \\ \theta_{z2}^m \\ \theta_{z3}^m \end{bmatrix} \quad (17)$$

The stiffness matrix (Eq. (16)) is expanded to add the fictitious stiffness (Eq. (17)) corresponding to nodal in-plane rotations. Hence, the expanded nodal displacements for nodal line  $i$  and  $m$ th harmonic is written as

$$\{\mathcal{D}_i^m\}^T = \{u_i^m \quad v_i^m \quad w_i^m \quad \theta_{xi}^m \quad \theta_{yi}^m \quad \theta_{zi}^m\} \quad (18)$$

The explicit form of the expanded stiffness matrix can be found in the Appendix A.1.

### 3.4 Geometric matrix and approach of general loading

The geometric matrix can be derived from the potential energy done by stresses through the nonlinear strains of the buckling displacements (Cheung 1976, Chu *et al.* 2005, Chu *et al.* 2006). For thin-walled members, we consider only longitudinal stresses and other types of stresses are supposed to be ignorable. The potential energy can be calculated as

$$W = \frac{t}{2} \int_0^a \int_0^b g(x, y, \sigma) \left[ \left( \frac{\partial u}{\partial y} \right)^2 + \left( \frac{\partial v}{\partial y} \right)^2 + \left( \frac{\partial w}{\partial y} \right)^2 \right] dx dy \quad (19)$$

where  $g(x, y, \sigma)$  is a function of co-ordinates  $(x, y)$  and the longitudinal stresses. It is assumed that this function can be expressed for a strip as

$$g(x, y, \sigma) = f_1(x, \sigma) f_2(y) \quad (20)$$

If the load is applied at the shear centre, the functions  $f_1(x, \sigma)$  and  $f_2(y)$  can be explicitly defined. The function  $f_1(x, \sigma)$  has a common form

$$f_1(x, \sigma) = \sigma_1 - (\sigma_1 - \sigma_2) \frac{x}{b} \quad (21)$$

where  $\sigma_1$  and  $\sigma_2$  are the compressive stresses (Fig. 1(b)).

The function  $f_2(y)$  depends on the type of loading and can be determined in some particular cases as written in Bui (2009).

With the defined functions  $f_1(x, \sigma)$  and  $f_2(y)$ , the element geometric matrix for each case of loading can be obtained by substituting Eqs. (2) into Eq. (19), for example: Schafer (1997) constructed the geometric matrix for cases where the longitudinal stresses are uniform, Chu *et al.* (2005) determined the geometric matrix for the case of uniform distributed loads applied at the shear centre and Bui (2009) formulated the geometric matrix for gradient moments; these authors developed their 2-nodal line finite strips based on the Kirchhoff plate theory. Note, in cases where the stress varies in the longitudinal direction, the element geometric stiffness matrices of different wave numbers are coupled each other and have the form

$$[K_G]_e = \begin{bmatrix} [K_G^{11}]_e & [K_G^{12}]_e & \dots & [K_G^{1r}]_e \\ [K_G^{21}]_e & [K_G^{22}]_e & \dots & [K_G^{2r}]_e \\ \dots & \dots & \dots & \dots \\ [K_G^{r1}]_e & [K_G^{r2}]_e & \dots & [K_G^{rr}]_e \end{bmatrix} \quad (22)$$

where  $[K_G^{mm}]_e$  is the geometric matrix associated with wave number  $m$ ,  $[K_G^{nm}]_e = [K_G^{mn}]_e$  is the coupled geometric matrix associated with wave number  $m$  and  $n$ .

However, in the practice, the loading is more complex; the section can be warped when the load is not applied at the shear centre. In these cases, the function  $f_2(y)$  is much more difficult to define. We apply the approach described in Bui (2009) to perform approximately the integration of Eq. (19) in a general loading condition; the strip is divided into cells in the longitudinal direction (Fig. 3). In a cell, the longitudinal stress is considered linear varying in the transverse direction and constant in the longitudinal direction. The potential energy (Eq. (19)) can be approximately determined by

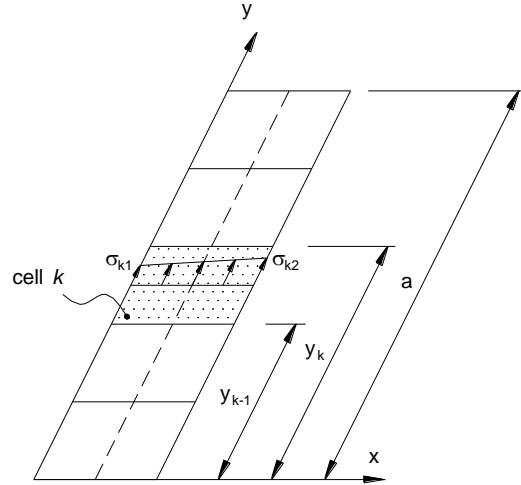


Fig. 3 Division of a strip in cells

$$W = \frac{t}{2} \sum_{k=1}^N \int_{y_{k-1}}^{y_k} \int_0^b \left[ \sigma_{1k} - (\sigma_{1k} - \sigma_{2k}) \frac{x}{b} \right] \left[ \left( \frac{\partial u}{\partial y} \right)^2 + \left( \frac{\partial v}{\partial y} \right)^2 + \left( \frac{\partial w}{\partial y} \right)^2 \right] dx dy \quad (23)$$

where  $N$  is the number of cells in the strip;  $\sigma_{1k}$  and  $\sigma_{2k}$  are the longitudinal stresses obtained from a linear analysis and recorded at the middle of the longitudinal sizes of the  $k$ th cell (Fig. 3);  $y_{k-1}$  and  $y_k$  (Eq. (23)) are the ordinates of the cell in the longitudinal direction. If the strip is equally divided into  $N$  cells,  $y_{k-1}$  and  $y_k$  are calculated as

$$y_{k-1} = (k-1) \frac{a}{N}, \quad y_k = k \frac{a}{N} \quad (24)$$

The element geometric matrix can be obtained by substituting Eq. (2) into Eq. (23). This geometric matrix has the same form of Eq. (22). The expression of  $[K_G^{mm}]_e$  and  $[K_G^{mn}]_e$  when the strip is divided into equal cells is given in the Appendix A.2.

The buckling problem can be solved by eigenvalue equations

$$[K] + \lambda [K_G] = 0 \quad (25)$$

where  $\lambda$  is a scaling factor related to the critical load.

#### 4. Numerical application

In order to illustrate the application and to provide a better grasp of the capabilities of the approaches presented in the previous sections, the buckling behaviour of U-section beam-column and I-section beam are analyzed. Only sufficiently long members are considered.

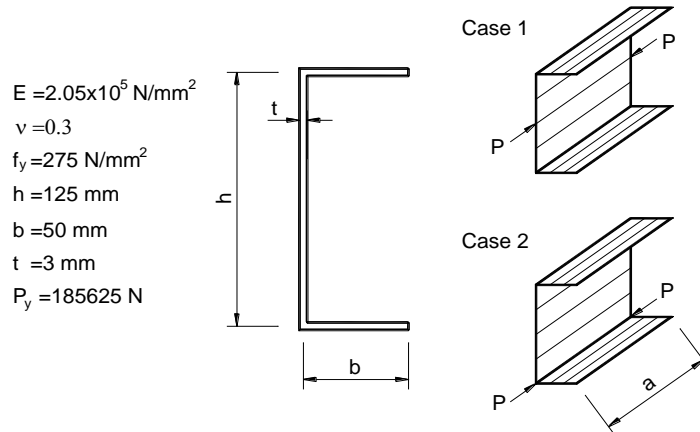


Fig. 4 U-section beam-column subjected to eccentric loads

Table 1 Buckling load of U-section beam-column ( $P_{cr}/P_y$ )

a (m)	Case 1			Case 2		
	FS	FE	Error (%)	FS	FE	Error (%)
1,0	0.7513(L)	0.7874(L)	-4.6	0.8752(FT)	0.8851(FT)	-1.1
2,0	0.4522(F)	0.4510(F)	0.3	0.2701(FT)	0.2679(FT)	0.8

Note: L- local buckling; F- flexural buckling; FT- flexural-torsional buckling

#### 4.1 Buckling of U-section beam-column under eccentric loads

The U-section beam-column under eccentric load is often found in structural trellis of cold-formed members. The dimensions of the U-section and the material properties are shown in Fig. 4. The section is modelled by 10 strips of 3-nodal lines: 3 strips for each flange, 4 strips for the web; 25 cells in longitudinal direction of the beam and 15 harmonics are used (the number of 3-nodal line strips utilized to model the section is suggested by a convergence study in Bui and Rondal (2008)). Two cases of load eccentricity are considered: for the case 1, the concentrated load applies at the middle of the height of the section and for the case 2 the concentrated load applies at the bottom corner. The critical stresses calculated by the 3-nodal line finite strip (FS) are compared with the results of 4-node finite element (FE), which is based on thick shell theory and implemented in the well-known program SAP2000 (2007). Table 1 indicates that the difference between the critical stresses analyzed by FS and FE model is insignificant. Both of FS and FE model give the same types of buckling mode shape. For example: when the length of the member is equal to 1,0m; in the case 1, we obtain the local buckling shape and in the case 2, we obtain the flexural-torsional buckling shape (Fig. 5).

#### 4.2 Buckling of I-section beam

The dimensions of the section and the material properties are shown in Fig. 6. The section is modelled by 10 strips of 3-nodal lines: 2 strips for each flange, 4 strips for the upper half of the web and 2 strips for the lower half; 25 cells in longitudinal direction of the beam and 25 harmonics are used. Fig. 7 shows the critical curves of the simply supported I-section beam subjected

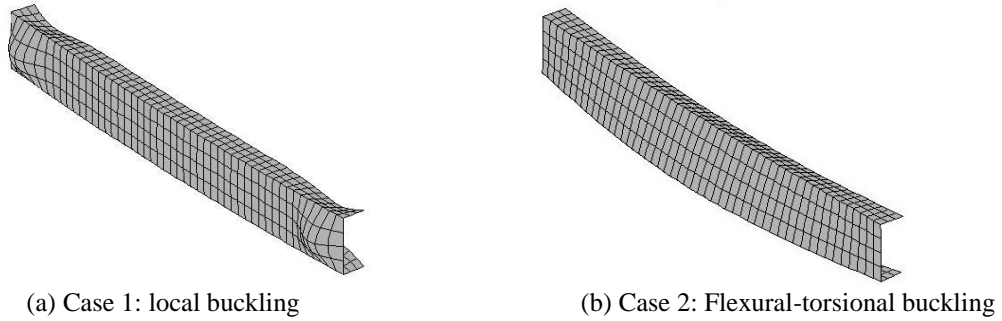


Fig. 5 Buckling shapes of beam-column when  $a=1,0m$

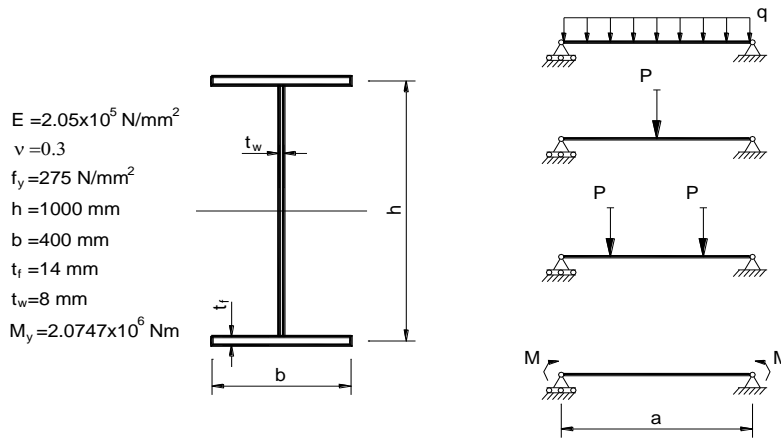


Fig. 6 I-section beam subjected to some types of loading

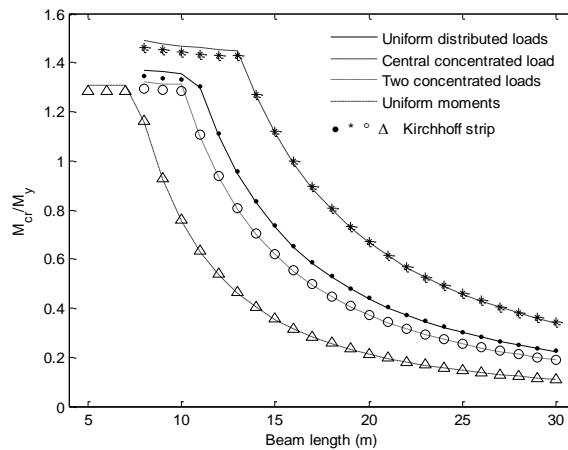


Fig. 7 Critical curves

respectively to uniform distributed loads, a central concentrated load, two concentrated loads at the one-fourths and uniform bending (Fig. 6). It can be seen that each curve has two distinct regions,

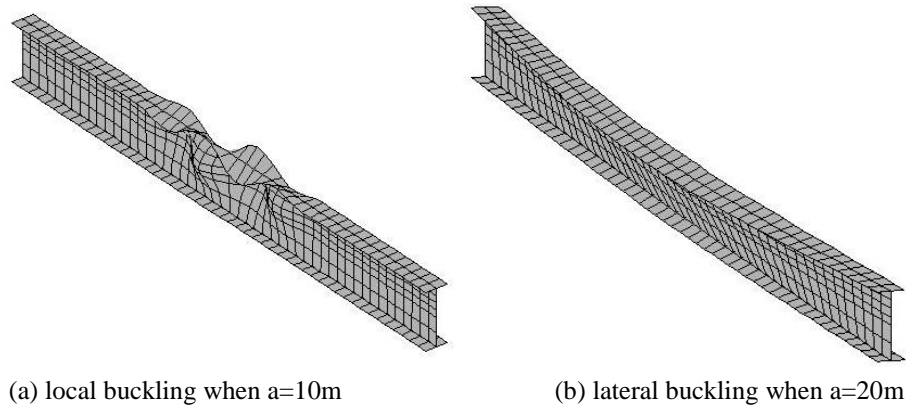


Fig. 8 Buckling shapes of beam under uniform distributed loads

which are corresponding to the local and the lateral buckling. The curves for the central concentrated load and the uniform bending represent the upper bound and lower bound, respectively. The critical moments of lateral loading for these two cases of loading are very different from the rest. The results analysed by 3-nodal line Mindlin-Reissner finite strip of this work are compared with those analysed by 2-nodal line Kirchhoff finite strip developed in Bui (2009). An excellent agreement between two types of strip can be seen in the lateral buckling region and a good agreement in the local buckling region. The buckling shapes of local and lateral buckling for the case of uniform distributed loads are showed in Fig. 8.

## 6. Conclusions

The buckling behaviour of thin-walled beam and beam-column subjected to arbitrary loads can be investigated using the 3-nodal line semi-analytical Mindlin-Reissner finite strip. This behaviour can be better understood through the critical curve which relates the minimal buckling stress with the length of the thin-walled member. The linear stiffness matrix and the geometric matrix of the strip are explicitly given in the Appendices. To implement the linear and geometric stiffness matrices, we use the in-plane rotation and general loading techniques. Because the strip with simply supported boundary conditions is developed then the linear stiffness is uncoupled while the geometric stiffness is coupled because normal stresses are varied along the length of the member. The very good agreement between the results analyzed by the Mindlin-Reissner finite strip, by the finite element and by the Kirchhoff finite strip demonstrates the reliability of the Mindlin-Reissner finite strip.

## Acknowledgements

This research was funded through a grant from the National Foundation for Science and Technology Development (NAFOSTED) of Vietnam. Their financial support is gratefully acknowledged.

## References

- Bradford, M.A. and Hancock, G.J. (1984), "Elastic interaction of local and lateral buckling in beams", *Thin-walled Structures*, **2**(1), 1-25.
- Bui, H.C. and Rondal, J. (2008), "Buckling analysis of thin-walled sections by semi-analytical Mindlin-Reissner finite strips – a treatment of drilling rotation problem", *Thin-walled Structures*, **46**, 646-652.
- Bui, H.C. (2009), "Buckling analysis of thin-walled sections under general loading conditions", *Thin-walled Structures*, **47**, 730-739.
- Cheung, Y.K. (1976), *Finite strip method in structural analysis*, Pergamon Press, New York.
- Chu, X.T., Ye, Z.M., Kettle, R. and Li, L.Y. (2005), "Buckling behaviour of cold-formed channel sections under uniformly distributed loads", *Thin-walled Structures*, **43**, 531-542.
- Chu, X.T., Ye, Z.M., Li, L.Y. and Kettle, R. (2006), "Local and distortional buckling of cold-formed zed-section beam under uniformly distributed transverse loads", *International Journal of Mechanical Sciences*, **48**(4), 378-388.
- Dawe, D.J., Lam, S.S.E. and Azizian, Z.G. (1993), "Finite strip post-local-buckling analysis of composite prismatic plate structures", *Computers & Structures*, **48**(6), 1011-1023.
- Hancock, G.J. (1978), "Local distortional and lateral buckling of I-beams", *Journal of the Structural Division*, ASCE, **104**(11), 1787-1798.
- Hinton, E. (1978), "Buckling of initially stressed Mindlin plates using a finite strip method", *Computers & Structures*, **8**, 99-105.
- Key, P.W. and Hancock, G.J. (1993), "A finite strip method for the elastic-plastic large displacement analysis of thin-walled and cold-formed steel sections", *Thin-walled Structures*, **16**, 3-29.
- Milašinović, D.D. (2011), "Geometric non-linear analysis of thin plate structures using the harmonic coupled finite strip method", *Thin-Walled Structures*, **49**(2), 280-290.
- Ovesy, H.R., Loughlan, J. and GhannadPour, S.A.M. (2005), "Geometric non-linear analysis of thin flat plates under end shortening, using different versions of the finite strip method", *International Journal of Mechanical Sciences*, **47**(12), 1923-1948.
- Ovesy, H.R., Loughlan, J., GhannadPour, S.A.M. and Morada, G. (2006), "Geometric non-linear analysis of box sections under end shortening, using three different versions of the finite-strip method", *Thin-Walled Structures*, **44**(6), 623-637.
- Ovesy, H.R., Loughlan, J. and GhannadPour, S.A.M. (2006), "Geometric non-linear analysis of channel sections under end shortening, using different versions of the finite strip method", *Computers & Structures*, **84**(13-14), 855-872.
- Schafer, B.W. (1997), "Cold-formed steel behaviour and design: analytical and numerical modelling of elements and members with longitudinal stiffeners", Ph. D. Dissertation, Cornell University, Ithaca, New York.
- SAP2000 (2007), *Structural analysis program, version 11.0*, Computers and Structures, Berkeley, California.
- Wang, S. and Dawe, D.J. (1996), "Finite strip large deflection and post-overall-buckling analysis of diaphragm-supported plate structures", *Computers & Structures*, **61**(1), 155-170.
- Zahari, R. and El-Zafrany, A. (2009), "Progressive failure analysis of composite laminated stiffened plates using the finite strip method", *Composite Structures*, **87**(1), 63-70.
- Mohri, F., Damil, N. and Potier-Ferry, M. (2012), "Pre-deflection effects on stability of thin-walled beams with open sections", *Steel and Composite Structures*, **13**(1), 71-89.

## Appendix

### A.1 The expanded stiffness matrix ( $K^m$ )

$$\begin{aligned}
K^m(1,1) &= \frac{Ct}{3} \left( \frac{7}{b} + \frac{b(k^m)^2(1-\nu)}{5} \right); & K^m(2,1) &= \frac{Ctk^m}{4} (3\nu - 1) \\
K^m(2,2) &= \frac{Ct}{3} \left( \frac{7(1-\nu)}{2b} + \frac{2b(k^m)^2}{5} \right); & K^m(3,3) &= D \left( \frac{7}{3b} + \frac{2b(k^m)^2}{15} \right) \\
K^m(4,3) &= -\frac{2Dbk^m}{15}; & K^m(4,4) &= \frac{Ct^3}{36} \left( \frac{7(1-\nu)}{2b} + \frac{2b(k^m)^2}{5} \right) + \frac{2Db}{15} \\
K^m(5,3) &= \frac{D}{2}; & K^m(5,4) &= \frac{Ct^3 k^m (3\nu - 1)}{48} \\
K^m(5,5) &= \frac{Ct^3}{36} \left( \frac{7}{b} + \frac{b(k^m)^2(1-\nu)}{5} \right) + \frac{2Db}{15}; & K^m(6,6) &= 19F \\
K^m(7,1) &= \frac{Ct}{3} \left( -\frac{8}{b} + \frac{b(k^m)^2(1-\nu)}{10} \right); & K^m(7,2) &= -\frac{Ctk^m(1+\nu)}{3} \\
K^m(7,7) &= \frac{4Ct}{3} \left( \frac{4}{b} + \frac{b(k^m)^2(1-\nu)}{5} \right); & K^m(8,1) &= -\frac{Ctk^m(1+\nu)}{3} \\
K^m(8,2) &= \frac{Ct}{3} \left( \frac{b(k^m)^2}{5} - \frac{4(1-\nu)}{b} \right); & K^m(8,8) &= \frac{8Ct}{3} \left( \frac{b(k^m)^2}{5} + \frac{(1-\nu)}{b} \right) \\
K^m(9,3) &= D \left( -\frac{8}{3b} + \frac{b(k^m)^2}{15} \right); & K^m(9,4) &= -\frac{Dbk^m}{15} \\
K^m(9,5) &= -\frac{2D}{3}; & K^m(9,9) &= D \left( \frac{16}{3b} + \frac{8b(k^m)^2}{15} \right) \\
K^m(10,3) &= -\frac{Dbk^m}{15}; & K^m(10,4) &= \frac{Ct^3}{36} \left( \frac{b(k^m)^2}{5} - \frac{4(1-\nu)}{b} \right) + \frac{Db}{15} \\
K^m(10,5) &= \frac{Ct^3 k^m (1+\nu)}{36}; & K^m(10,9) &= -\frac{8Dbk^m}{15} \\
K^m(10,10) &= \frac{2Ct^3}{9} \left( \frac{b(k^m)^2}{5} + \frac{(1-\nu)}{b} \right) + \frac{8Db}{15}; & K^m(11,3) &= \frac{2D}{3} \\
K^m(11,4) &= -\frac{Ct^3 k^m (1+\nu)}{36}; & K^m(11,5) &= \frac{Ct^3}{36} \left( -\frac{8}{b} + \frac{b(k^m)^2(1-\nu)}{10} \right) + \frac{Db}{15} \\
K^m(11,11) &= \frac{Ct^3}{9} \left( \frac{4}{b} + \frac{b(k^m)^2(1-\nu)}{5} \right) + \frac{8Db}{15}; & K^m(12,6) &= -8F \\
K^m(12,12) &= 16F; & K^m(13,1) &= \frac{Ct}{3} \left( \frac{1}{b} - \frac{b(k^m)^2(1-\nu)}{20} \right) \\
K^m(13,2) &= \frac{Ctk^m(1+\nu)}{12}; & K^m(13,7) &= \frac{Ct}{3} \left( -\frac{8}{b} + \frac{b(k^m)^2(1-\nu)}{10} \right)
\end{aligned}$$

$$\begin{aligned}
K^m(13,8) &= -\frac{Ctk^m(1+\nu)}{3} ; K^m(13,13) = \frac{Ct}{3} \left( \frac{7}{b} + \frac{b(k^m)^2(1-\nu)}{5} \right) \\
K^m(14,1) &= -\frac{Ctk^m(1+\nu)}{12} ; K^m(14,2) = \frac{Ct}{6} \left( -\frac{b(k^m)^2}{5} + \frac{(1-\nu)}{b} \right) \\
K^m(14,7) &= \frac{Ctk^m(1+\nu)}{3} ; K^m(14,8) = \frac{Ct}{3} \left( \frac{b(k^m)^2}{5} - \frac{4(1-\nu)}{b} \right) \\
K^m(14,13) &= \frac{Ctk^m(1-3\nu)}{4} ; K^m(14,14) = \frac{Ct}{3} \left( \frac{2b(k^m)^2}{5} + \frac{7(1-\nu)}{2b} \right) \\
K^m(15,3) &= D \left( \frac{1}{3b} - \frac{b(k^m)^2}{30} \right) ; K^m(15,4) = \frac{Dbk^m}{30} \\
K^m(15,5) &= \frac{D}{6} ; K^m(15,9) = D \left( -\frac{8}{3b} + \frac{b(k^m)^2}{15} \right) \\
K^m(15,10) &= -\frac{Dbk^m}{15} ; K^m(15,11) = -\frac{2D}{3} \\
K^m(15,15) &= D \left( \frac{7}{3b} + \frac{2b(k^m)^2}{15} \right) ; K^m(16,3) = \frac{Dbk^m}{30} \\
K^m(16,4) &= \frac{Ct^3}{72} \left( -\frac{b(k^m)^2}{5} + \frac{(1-\nu)}{b} \right) - \frac{Db}{30} ; K^m(16,5) = -\frac{Ct^3k^m(1+\nu)}{144} \\
K^m(16,9) &= -\frac{Dbk^m}{15} ; K^m(16,10) = \frac{Ct^3}{36} \left( \frac{b(k^m)^2}{5} - \frac{4(1-\nu)}{b} \right) + \frac{Db}{15} \\
K^m(16,11) &= \frac{Ct^3k^m(1+\nu)}{36} ; K^m(16,15) = -\frac{2Dbk^m}{15} \\
K^m(16,16) &= \frac{Ct^3}{36} \left( \frac{2b(k^m)^2}{5} + \frac{7(1-\nu)}{2b} \right) + \frac{2Db}{15} ; K^m(17,3) = -\frac{D}{6} \\
K^m(17,4) &= \frac{Ct^3k^m(1+\nu)}{144} ; K^m(17,5) = \frac{Ct^3}{36} \left( \frac{1}{b} - \frac{b(k^m)^2(1-\nu)}{20} \right) - \frac{Db}{30} \\
K^m(17,9) &= \frac{2D}{3} ; K^m(17,10) = -\frac{Ct^3k^m(1+\nu)}{36} \\
K^m(17,11) &= \frac{Ct^3}{36} \left( -\frac{8}{b} + \frac{b(k^m)^2(1-\nu)}{10} \right) + \frac{Db}{15} ; K^m(17,15) = -\frac{D}{2} \\
K^m(17,16) &= \frac{Ct^3k^m(1-3\nu)}{48} ; K^m(17,17) = \frac{Ct^3}{36} \left( \frac{7}{b} + \frac{b(k^m)^2(1-\nu)}{5} \right) + \frac{2Db}{15} \\
K^m(18,6) &= -11F ; K^m(18,12) = -8F ; K^m(18,18) = 19F
\end{aligned}$$

where

$$k^m = \frac{m\pi}{a} ; C = \frac{Ea}{2(1-\nu^2)} ; D = \frac{5}{6} \frac{Gta}{2} ; F = \frac{Gtab}{360}$$

## A.2 The coupled geometric matrix ( $K_G^{mn}$ ) for the case of general loading condition

$$\begin{aligned}
K_G^{mn}(1,1) &= C \sum_{k=1}^N (7\sigma_{1k} + \sigma_{2k}) I_{ck} ; & K_G^{mn}(2,2) &= C \sum_{k=1}^N (7\sigma_{1k} + \sigma_{2k}) I_{sk} \\
K_G^{mn}(3,3) &= C \sum_{k=1}^N (7\sigma_{1k} + \sigma_{2k}) I_{ck} ; & K_G^{mn}(7,1) &= C \sum_{k=1}^N 4\sigma_{1k} I_{ck} \\
K_G^{mn}(7,7) &= C \sum_{k=1}^N 16(\sigma_{1k} + \sigma_{2k}) I_{ck} ; & K_G^{mn}(8,2) &= C \sum_{k=1}^N 4\sigma_{1k} I_{sk} \\
K_G^{mn}(8,8) &= C \sum_{k=1}^N 16(\sigma_{1k} + \sigma_{2k}) I_{sk} ; & K_G^{mn}(9,3) &= C \sum_{k=1}^N 4\sigma_{1k} I_{ck} \\
K_G^{mn}(9,9) &= C \sum_{k=1}^N 16(\sigma_{1k} + \sigma_{2k}) I_{ck} ; & K_G^{mn}(13,1) &= C \sum_{k=1}^N -(\sigma_{1k} + \sigma_{2k}) I_{ck} \\
K_G^{mn}(13,7) &= C \sum_{k=1}^N 4\sigma_{2k} I_{ck} ; & K_G^{mn}(13,13) &= C \sum_{k=1}^N (\sigma_{1k} + 7\sigma_{2k}) I_{ck} \\
K_G^{mn}(14,2) &= C \sum_{k=1}^N -(\sigma_{1k} + \sigma_{2k}) I_{sk} ; & K_G^{mn}(14,8) &= C \sum_{k=1}^N 4\sigma_{2k} I_{sk} \\
K_G^{mn}(14,14) &= C \sum_{k=1}^N (\sigma_{1k} + 7\sigma_{2k}) I_{sk} ; & K_G^{mn}(15,3) &= C \sum_{k=1}^N -(\sigma_{1k} + \sigma_{2k}) I_{ck} \\
K_G^{mn}(15,9) &= C \sum_{k=1}^N 4\sigma_{2k} I_{ck} ; & K_G^{mn}(15,15) &= C \sum_{k=1}^N (\sigma_{1k} + 7\sigma_{2k}) I_{ck}
\end{aligned}$$

where  $N$  is the number of equal cells in the longitudinal direction of the strip;

$$\begin{aligned}
C &= \frac{tbmn\pi^2}{60a} \\
I_{ck} &= \frac{1}{a} \int_{\frac{(k-1)a}{N}}^{\frac{ka}{N}} \cos \frac{m\pi y}{a} \cos \frac{n\pi y}{a} dy \\
&= \begin{cases} \frac{1}{2N} + \frac{1}{4m\pi} \left[ \sin \frac{2m\pi k}{N} - \sin \frac{2m\pi(k-1)}{N} \right] & \text{if } m = n \\ \frac{1}{2\pi} \left[ \frac{1}{m+n} \left( \sin \frac{(m+n)\pi k}{N} - \sin \frac{(m+n)\pi(k-1)}{N} \right) + \frac{1}{m-n} \left( \sin \frac{(m-n)\pi k}{N} - \sin \frac{(m-n)\pi(k-1)}{N} \right) \right] & \text{if } m \neq n \end{cases} \\
I_{sk} &= \frac{1}{a} \int_{\frac{(k-1)a}{N}}^{\frac{ka}{N}} \sin \frac{m\pi y}{a} \sin \frac{n\pi y}{a} dy \\
&= \begin{cases} \frac{1}{2N} - \frac{1}{4m\pi} \left[ \sin \frac{2m\pi k}{N} - \sin \frac{2m\pi(k-1)}{N} \right] & \text{if } m = n \\ -\frac{1}{2\pi} \left[ \frac{1}{m+n} \left( \sin \frac{(m+n)\pi k}{N} - \sin \frac{(m+n)\pi(k-1)}{N} \right) - \frac{1}{m-n} \left( \sin \frac{(m-n)\pi k}{N} - \sin \frac{(m-n)\pi(k-1)}{N} \right) \right] & \text{if } m \neq n \end{cases}
\end{aligned}$$

Note: The matrices  $(K^m)$  and  $(K_G^{mn})$  are symmetric and of dimensions  $18 \times 18$

$$K^m(i, j) = K^m(j, i)$$

$$K_G^{mn}(i, j) = K_G^{mn}(j, i)$$

Other components of these matrices which are not written are equal to zero.